Synthesis, structure and antiferromagnetic behaviour of brannerite MnV_2O_6

Zhou Chuan-Cang(周传仓), Liu Fa-Min(刘发民)†, Ding Peng(丁 芃), Cai Lu-Gang(蔡鲁刚), Zhong Wen-Wu(钟文武), and Zhang Huan(张 嬛)

School of Physics and Nuclear Energy Engineering, Beijing University of Aeronautics and Astronautics, Beijing 100191, *China*

(Received 29 October 2009; revised manuscript received 21 December 2009)

Brannerite MnV_2O_6 with plate-like shape is successfully synthesized by hydrothermal method. Its crystal structure and morphology are investigated by x-ray diffraction (XRD), scanning electron microscopy (SEM), transmission electron microscope (TEM), high resolution transmission electron microscopy (HRTEM) and select area electronic diffraction (SAED). The results show that the brannerite MnV_2O_6 with monoclinic structure has a uniform plate-like shape with a diameter of about 5–8 μm and a thickness of about 500 nm. SAED patterns further confirm the structure of the brannerite MnV_2O_6 and the single crystalline character of the plate crystal. Magnetic properties are measured by superconducting quantum interference device (SQUID) in a temperature range of 2–300 K under a magnetic field of 1 T. The magnetic measurement results indicate that the material undergoes an antiferromagnetic transition with a Néel temperature of 17 K. Above 50 K, the inverse susceptibility is fitted well to the Curie–Weiss law with a calculated moment of 5.98 μ_B. Finally, the origin of antiferromagnetic behaviour in the brannerite MnV_2O_6 is explained by means of Anderson model.

Keywords: brannerite MnV_2O_6, hydrothermal synthesis, antiferromagnetic behaviour

PACC: 7550E, 8110D, 8116

1. Introduction

The MV_2O_6 compounds (monoclinic for M = Mn; triclinic for M = Co, Ni, Cu) with brannerite (UTi_2O_6) structure have been increasingly concerned as a kind of low-dimensional magnetic system.[1−10] The magnetic properties of CuV_2O_6 were also widely investigated.[11−13] MnV_2O_6 as a kind of new cathode material was extensively studied.[14] However, only Simon *et al.* studied disrupted antiferromagnetism in the brannerite MnV_2O_6 with long-range order.[8] The origin of antiferromagnetic behaviour in the brannerite MnV_2O_6 still needs to be discussed. The brannerite MnV_2O_6 is composed of VO_6 octahedral which shares opposite corners forming chains in the direction parallel to the b-axis. The VO_6 octahedral in adjacent chains shares the edges forming anion sheets in the direction parallel to the (001) planes. Mn ions are situated between anionic sheets so that each Mn ion is coordinated by six oxygen atoms arranged in a distorted octahedron. MnO_6 shares edges forming chains in parallel to the b-axis. These chains are not linked with each other and provide a rather open structure between the VO_6 sheets.

A lot of synthetic means have been developed to prepare vanadates with various sizes and morphologies.[9,10,15−17] Among various conventional synthetic routes, hydrothermal method, as a wet chemistry method, offers many advantages compared with usual methods. One of the main advantages is that the hydrothermal synthetic route can directly obtain highly crystallized powders with uniform grain size-distribution and high purity. Up to now, several synthesis methods of synthesising MnV_2O_6 such as solid-state reactions[18] and wet chemical methods,[14] have been reported. However, there are only two reports of the hydrothermal synthesis of MnV_2O_6. Liu *et al.* reported on the hydrothermal synthesis of the MnV_2O_6 nanobelts.[18] Inagaki *et al.* also prepared the MnV_2O_6 crystal with rod-like shape under autogenous hydrothermal condition.[19] The synthesis of two-dimensional plate-like MnV_2O_6 has never been reported before. In the present paper, a facile process is reported to fabricate plate-like anhydrous MnV_2O_6 by the hydrothermal treatment of $Mn(NO_3)_2$ solution and Na_3VO_4 powders without using any tem-

†Corresponding author. E-mail: fmliu@buaa.edu.cn

© 2010 Chinese Physical Society and IOP Publishing Ltd

plates and surfactants. Furthermore, its structure and magnetic properties are studied by x-ray diffraction (XRD), scanning electron microscope (SEM), transmission electron microscope (TEM), high resolution transmission electron microscopy (HRTEM), select area electronic diffraction (SAED) and MPMS SQUID magnetometer, where MPSM and SQUID stand for magnetic property measurement system and superconducting quantum interference device respectively. Finally, the origin of antiferromagnetic behaviour in the brannerite MnV_2O_6 is explained by the Anderson model.

2. Experiment

All analytical purity reagents in this experiment were purchased from Beijing Chemical Reagents Company and used without further purification. Firstly, 1.79-g 50% $Mn(NO_3)_2$ solution and 4-g Na_3VO_4 powders were put into beakers with 20-ml distilled water separately. After that, the solution of $Mn(NO_3)_2$ solution was added slowly into the Na_3VO_4 solution and the mixture was vigorously magnetic stirred in room atmosphere for 30 min to form homogenous solution, in which a small amount of nitric acid or ammonia water was added drop by drop to promote solution gel till the pH value of the solution was about 7.0. Subsequently, the suspension solution was transferred into a 50-ml Teflon lined stainless steel autoclave. Then the autoclave was sealed and maintained at 180 °C for 48 h and cooled down to room temperature in air. Finally, the brown slurry products were filtered, washed several times with distilled water and absolute alcohol to remove ions possibly remaining in the final products, and finally dried at 80 °C in air for 5 h for further characterization.

The XRD patterns of the samples were collected at room temperature in a 2θ range from 10° to 90° in steps of 0.02° and a fixed counting time of 4 s by using an X′Pert pro MPD XRD system with Cu Kα radiation, a voltage of 40 kV and a current of 40 mA. The morphology of sample surface was determined by an SEM image, and the concentration of element content was measured from an energy dispersive spectrometer (EDS) image, taken with an FEI-SIRION scanning electronic microanalyzer. TEM micrographs, HRTEM pattern and SAED pattern were obtained on PHILIPS-CM200 and JEM-2010 type TEM. Magnetic susceptibility in a temperature range of 2–300 K was measured in a magnetic field of 1 T by an MPMS XL-7 SQUID magnetometer.

3. Results and discussion

The XRD pattern of the sample is shown in Fig. 1. The main diffraction peaks in Fig. 1 can be readily indexed as monoclinic MnV_2O_6 (space group: $C2/m$) with an end-centred lattice, which accord with the reported values (JCPDS card NO.35-0139).[20] The lattice constant can be calculated according to the crystal-plane distance formula of monoclinic symmetry

$$d = \frac{1}{\sqrt{\dfrac{\left(\dfrac{h}{a}\right)^2 + \left(\dfrac{l}{c}\right)^2 + \dfrac{2hl\cos\beta}{ac}}{\sin\beta} + \left(\dfrac{k}{b}\right)^2}}, \quad (1)$$

where d is the interplanar distance, h, k, l are the crystal plane index, a, b, c, β are the lattice parameters. The values of lattice constants can be calculated to be $a = 0.9318$ nm, $b = 0.3536$ nm, $c = 0.6765$ nm, and $\beta = 112.391°$. These obtained values basically conform to the previously reported results by Sung-Soo Kim *et al.*,[14] i.e. $a = 0.9303$ nm, $b = 0.3536$ nm, $c = 0.6756$ nm, and $\beta = 112.388°$. It is considered that these observed delicate differences are caused by the slight change in oxygen content.

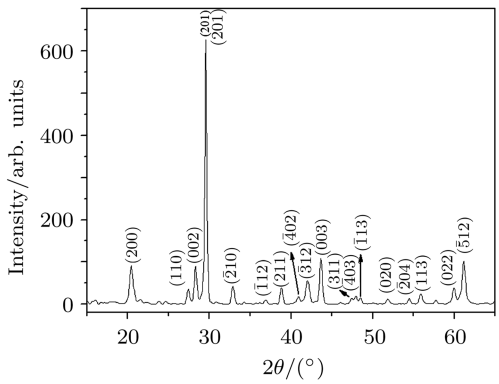


Fig. 1. The x-ray diffraction pattern of MnV_2O_6.

Figure 2 shows an SEM image of the as-obtained MnV_2O_6. The sample has a uniform plate-like shape with a diameter of about 5–8 μm and a thickness of about 500 nm. A lot of plates are arrayed together to form a series of clusters with flower-like shapes. In addition, the EDS spectrum of MnV_2O_6 crystals (shown in Fig. 3) confirms that no other metal elements were detected except for Mn and V. The molar

ratio of Mn:V:O was calculated to be approximately 1:2:6, which is accordant with the formula of MnV_2O_6.

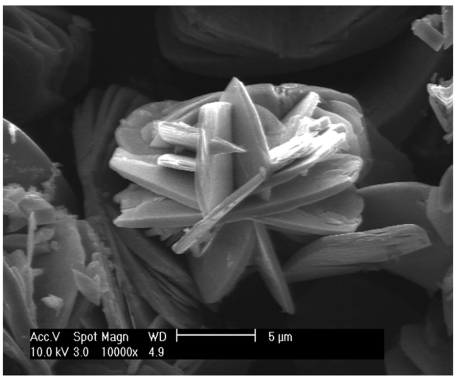


Fig. 2. The SEM image of MnV_2O_6 synthesized by hydrothermal method.

Figures 4(a) and 4(b) show the TEM and the HRTEM images of as-prepared MnV_2O_6, respectively. The TEM image further demonstrates that the obtained product has a uniform plate-like shape and particle size. The HRTEM image, which is taken from the single plate, shows that the plate crystal has clearly resolved lattice fringes and the inter-planar spacing is measured to be 0.437 nm, which corresponds to the (101) plane of MnV_2O_6. Figure 4(c) shows the SAED pattern of as-prepared MnV_2O_6. The SAED patterns are easily indexed on the basis of a monoclinic cell, which are in agreement with the data on the XRD pattern. And the SAED pattern reveals the single crystalline character of the plate crystal. All these results prove that the MnV_2O_6 prepared by a hydrothermal method is directionally grown and has crystalline integrality.

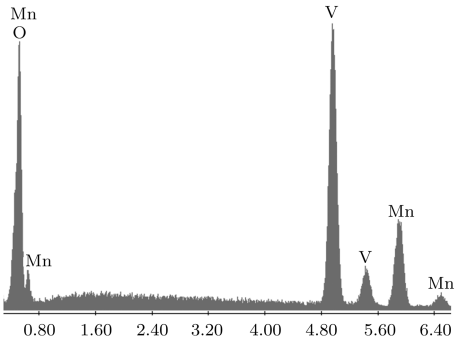


Fig. 3. The EDS spectrum of MnV_2O_6 synthesized by hydrothermal method.

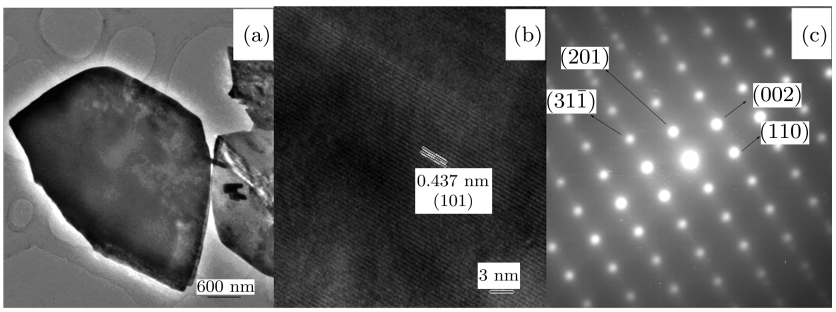


Fig. 4. The TEM image (a), HRTEM image (b), SAED pattern (c) of MnV_2O_6 prepared by hydrothermal synthesis.

Figure 5 shows χ–T curve and $1/\chi$–T curve in an applied field of 1 T for the brannerite MnV_2O_6. The χ–T curve is characterized by a maximum at 17 K and a maximum molar susceptibility $\chi_{\rm mol}$ = 0.189 emu/mol, which is very similar to the result reported by Simon *et al.*[8] Therefore, the material undergoes an antiferromagnetic–paramagnetic transition with a Néel temperature of 17 K. Below 17 K a kink appears at T = 11.1 K which gives rise to a sharp λ-type anomaly. It was ascribed to the onset of long range antiferromagnetic ordering. For the crystal the paramagnetic defect concentration was estimated from the low temperature paramagnetic tail to be below 0.9% of all cation sites. These results are similar to the previously reported antiferromagnetic spin-chain behaviour of the CuV_2O_6.[12] Above 50 K, the inverse susceptibility is fitted well to the Curie–Weiss law $\chi_{\rm m} = C/(T-\theta)$. The calculated paramagnetic Weiss temperature is positive (θ = 5.5 K), indicating that significant ferromagnetic exchange interactions are present above $T_{\rm N}$. According to formula (2), the effective magnetic moment $\mu_{\rm eff}$ of the brannerite MnV_2O_6 can be calculated with the value of

$C = 4.146$ K emu mol-f.u.$^{-1}$

$$\mu_{\rm eff}=\frac{1}{\mu_{\rm B}}\sqrt{\frac{3C\kappa_{\rm B}}{N}}, \tag{2}$$

where C is the Curie constant, $\kappa_{\rm B}$ is the Boltzmann's constant, $\mu_{\rm B}$ is the Bohr magneton, and N is the number of magnetic ions.

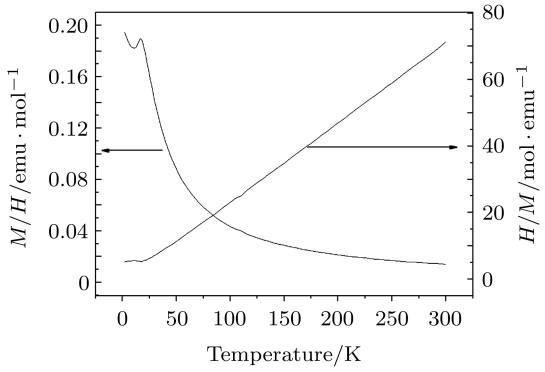


Fig. 5. Magnetic susceptibility and inverse susceptibility of the brannerite MnV_2O_6 each as a function of temperature. These values are measured under an applied field of 1 T.

The calculated effective magnetic moment $\mu_{\rm eff}$ is 5.98 $\mu_{\rm B}$, which is close to the spin-only value 5.92 $\mu_{\rm B}$ as expected for $S = 5/2$ where the Lande's g-factor might be expected to be 2.

Mn^{2+} ions are isolated by the distorted octahedron VO_6 sheets which are parallel to crystal plane (001) so that the direct interaction between Mn^{2+} ions cannot take place. According to the Anderson model, there exists a superexchange interaction between Mn^{2+} ions by means of oxygen ion. And two 2p electrons of oxygen ion participate in the exchange process. If the ground state Mn^{2+}–O^{2-}–Mn^{2+} is excited, the electron transition occurs from the O^{2-} p′ states to neighbouring Mn^{2+} d states and the other electronic states Mn^{+}–O–Mn^{2+} turn up, so O^{2-} p″ electron with the net spin, which is matched pair with O^{2-} p′ in the ground state, has a direct exchange interaction with Mn^{2+} d_2 electron. Different coordinations of Mn^{2+} 3d electronic wave function and O^{2-} 2p electronic wave function and crystal field have a great effect on the p–d electron exchange interaction. Only when 3d electron orbit is non-orthogonal to 2p orbit, can 2p electron hop into the adjacent 3d orbit of Mn^{2+}. When 3d orbit is orthogonal to 2p orbit, the direct exchange integral (J) between O^{2-} 2p and Mn^{2+} 3d is positive. When 3d orbit is non-orthogonal to 2p orbit, $J < 0$ can be obtained. Due to the dumbbell shape of 2p electronic orbit of O^{2-}, the bond angle of Mn^{2+}–O^{2-}–Mn^{2+} is 180° and the electron mobility reaches maximum. Among the three kinds of p–d orbit non-orthogonal states, the bond angle between p_z and $d_{3z^2-r^2}$ is 180°, in which case $J < 0$. We speculate that the electron transition occurs in a low temperature range and the direct exchange integral J is negative. While, direct exchange integral has a crucial effect on the indirect exchange integral.

Indirect exchange integral:

$$A = \left[\frac{1}{E(\uparrow\downarrow)^2} - \frac{1}{E(\uparrow\uparrow)^2}\right] b^2 J, \tag{3}$$

where $E(\uparrow\downarrow)$ and $E(\uparrow\uparrow)$ are the increased energies for the electronic transition from electronic p state to electronic d state corresponding to the cases of $(d_1 d'_1)^1$ and $(d_1 d'_1)^3$ respectively; b is the electron transition integral; J is the direct exchange integral between O^{2-} 2p′ electron and Mn^{2+} $3d_2$ electron (J is actually a sum of p′–d transition energy and direct exchange energy between d_1 and d'_1).

Indirect exchange integral is related to two physical processes, one is electronic transition from 2p orbit of O^{2-} to 3d orbit of Mn^{2+}, the other is the direct exchange interaction between p″ electron and d_2 electron. Due to Mn^{2+} 3d electrons in a half-filled shell, $E(\uparrow\downarrow) \ll E(\uparrow\uparrow)$, finally $A = b^2 J/E(\uparrow\downarrow)^2$ is obtained. According to Hersenberg's theory, if $A > 0$, for a stable spin state all electrons spin in parallel, thereby inducing a spontaneous magnetic moment, which is also the origin of ferromagnetism. However, if $A < 0$, for the stable state the neighbouring electron spins are antiparallel to each other, so there exists no spontaneous magnetic moment, thus resulting in antiferromagnetism. We speculate that J is negative when there exists a superexchange interaction between Mn^{2+} ions in a low temperature range. Therefore, indirect exchange integral A is also negative and the brannerite MnV_2O_6 is antiferromagnet in a low temperature range.

4. Conclusions

A facile hydrothermal method is successfully developed to prepare the brannerite MnV_2O_6. The SEM and the TEM images indicate that the MnV_2O_6 has a uniform plate-like shape with a diameter of about 5–8 μm and a thickness of about 500 nm. The clearly

resolved lattice fringes in HRTEM image show that the plate crystal has a good crystalline integrality. The SAED pattern further demonstrates the MnV_2O_6 crystal structure and the single crystalline character of the plate crystal. The magnetic measurements indicate that the brannerite MnV_2O_6 undergoes an antiferromagnetic transition with a Néel temperature of 17 K. Above 50 K, the inverse susceptibility is fitted well to the Curie–Weiss law $\chi_m = C/T - \theta$ with a calculated moment of 5.98 μ_B, which is in agreement with the expected spin value for Mn^{2+} (5.92 μ_B). The calculated paramagnetic Weiss temperature is positive ($\theta = 5.5$ K), indicating that the significant ferromagnetic exchange interactions are present above T_N. According to the Anderson model, the MnV_2O_6 is antiferromagnet in a low temperature range, which is induced by the superexchange interaction of Mn^{2+}–O^{2-}–Mn^{2+}.

References

[1] Hase M, Terasaki I and Uchinokura K 1993 *Phys. Rev. Lett.* **70** 3651

[2] Uchiyama Y, Sasago Y, Tsukada I, Uchinokura K, Zheludev A, Hayashi T, Miura N and Boni P 1999 *Phys. Rev. Lett.* **83** 632

[3] Bieringer M, Greedan J E and Luke G M 2000 *Phys. Rev.* B **62** 6521

[4] Goossens D J, Studer A J, Kennedy S J and Hicks T J 2000 *J. Phys.*: *Condens. Matter* **12** 4233

[5] Ronnow H M, Wildes A R and Bramwell S T 2000 *Physica* B **676** 276

[6] Jiang Z J and Mo D 2000 *Chin. Phys.* **9** 290

[7] James M and Watson J N 2002 *J. Solid State Chem.* **165** 261

[8] Simon A, Kimber J and AttField J Paul 2007 *Phys. Rev.* B **75** 064406

[9] Wei Y J, Kyung Wan Nam, Chen G, Chang Wan Ryu and Kwang Bum Kim 2005 *Solid State Ionics* **176** 2243

[10] Zhou C C, Liu F M and Ding P 2009 *Chin. Phys.* B **18** 5055

[11] Belaiche M, Bakhache M and Drillon M 2001 *Physica* B **305** 270

[12] Prokofiev A V, Kremer R K and Assmus W 2001 *J. Cryst. Growth* **231** 498

[13] Vasilev A N, Ponomarenko L A, Antipov E V, Velikodny Yu A, Smirnov A I, Isobe M and Ueda Y 2000 *Physica* B **284** 1615

[14] Kim S S, Hiromasa I and Masataka Wakihara 2001 *Solid State Ionics* **139** 57

[15] Yusaku Takita, Susumu Hikazudani, Kazuya Soda and Katsutoshi Nagaoka 2008 *J. Mol. Catal.* A: *Chem.* **280** 164

[16] Wang X J, Fei Y J, Xiong Y Y, Nie Y X, Feng K A and Li L D 2002 *Chin. Phys.* **11** 737

[17] Krzysztof Moca and Jacek Ziókowski 1987 *J. Solid State Chem.* **69** 299

[18] Liu Y, Zhang Y G, Duan J, Yu W C and Qian Y T 2006 *J. Cryst. Growth* **291** 320

[19] Michio Inagaki, Takahiro Morishita, Masanori Hirano, Vinay Gupta and Tsuyoshi Nakajima 2003 *Solid State Ionics* **156** 275

[20] Kozlowski R, Ziolkowski J and Kozlowska A 1980 *J. Solid State Chem.* **35** 1